

Insulin Signaling in Bupivacaine-induced Cardiac Toxicity

Sensitization during Recovery and Potentiation by Lipid Emulsion

Michael R. Fettiplace, M.S., Katarzyna Kowal, B.S., Richard Ripper, C.V.T., Alexandria Young, B.S., Kinga Lis, B.S., Israel Rubinstein, M.D., Marcelo Bonini, Ph.D., Richard Minshall, Ph.D., Guy Weinberg, M.D.

ABSTRACT

Background: The impact of local anesthetics on the regulation of glucose homeostasis by protein kinase B (Akt) and 5'-adenosine monophosphate-activated protein kinase (AMPK) is unclear but important because of the implications for both local anesthetic toxicity and its reversal by IV lipid emulsion (ILE).

Methods: Sprague-Dawley rats received 10 mg/kg bupivacaine over 20 s followed by nothing or 10 ml/kg ILE (or ILE without bupivacaine). At key time points, heart and kidney were excised. Glycogen content and phosphorylation levels of Akt, p70 s6 kinase, s6, insulin receptor substrate-1, glycogen synthase kinase-3 β , AMPK, acetyl-CoA carboxylase, and tuberous sclerosis 2 were quantified. Three animals received Wortmannin to irreversibly inhibit phosphoinositide-3-kinase (Pi3k) signaling. Isolated heart studies were conducted with bupivacaine and LY294002—a reversible Pi3K inhibitor.

Results: Bupivacaine cardiotoxicity rapidly dephosphorylated Akt at S473 to $63 \pm 5\%$ of baseline and phosphorylated AMPK to $151 \pm 19\%$. AMPK activation inhibited targets downstream of mammalian target of rapamycin complex 1 *via* tuberous sclerosis 2. Feedback dephosphorylation of IRS1 to $31 \pm 8\%$ of baseline sensitized Akt signaling in hearts resulting in hyperphosphorylation of Akt at T308 and glycogen synthase kinase-3 β to $390 \pm 64\%$ and $293 \pm 50\%$ of baseline, respectively. Glycogen accumulated to $142 \pm 7\%$ of baseline. Irreversible inhibition of Pi3k upstream of Akt exacerbated bupivacaine cardiotoxicity, whereas pretreating with a reversible inhibitor delayed the onset of toxicity. ILE rapidly phosphorylated Akt at S473 and T308 to $150 \pm 23\%$ and $167 \pm 10\%$ of baseline, respectively, but did not interfere with AMPK or targets of mammalian target of rapamycin complex 1.

Conclusion: Glucose handling by Akt and AMPK is integral to recovery from bupivacaine cardiotoxicity and modulation of these pathways by ILE contributes to lipid resuscitation. (ANESTHESIOLOGY 2016; 124:428-42)

BUPIVACAINE toxicity is an uncommon but life-threatening event.^{1,2} If toxicity occurs in the clinical setting, an infusion of IV lipid emulsion (ILE) is used to accelerate recovery. The mechanism of ILE-based reversal of toxicity includes both a scavenging effect and a direct effect that improves cardiac output.³ This improvement of cardiac output is seen in the absence of toxicity⁴ and contributes to the rapid recovery from toxicity.⁵ However, the cellular signaling underlying this effect is unknown. Recent reports demonstrate that bupivacaine disrupts targets of classical insulin signaling,⁶ including protein kinase B (Akt) and ribosomal protein s6 kinase 1, in cellular models.^{7,8} Furthermore, the amide-linked local anesthetics, ropivacaine and lidocaine, disrupt the assembly of phosphoinositide-3-kinase (Pi3k), thereby blocking phosphorylation of Akt,⁹ an effect that is independent of classical sodium channel blockade.¹⁰ Beyond Akt, bupivacaine activates other controllers of glucose homeostasis, including 5'-adenosine monophosphate-activated protein kinase (AMPK),^{11,12} an effect that may

What We Already Know about This Topic

- IV lipid emulsion reduces local anesthetic toxicity
- *In vitro*, local anesthetics alter phosphorylation in kinase signaling related to glucose metabolism
- Glucose metabolism influences toxicity in the heart and other tissues

What This Article Tells Us That Is New

- *In vivo*, local anesthetic toxicity altered phosphorylation at targets of glucose metabolism, including Akt, 5'-adenosine monophosphate-activated protein kinase, and insulin receptor substrate-1
- IV lipid emulsion reduced these local anesthetic-induced changes in phosphorylation

provide cytoprotection during toxicity.¹³ Conversely, ILE and other fatty acids increase phosphorylation of Akt and other canonical insulinergic targets when used as an adjuvant in recovery from ischemia-reperfusion injury.¹⁴⁻¹⁸ In

Submitted for publication April 28, 2015. Accepted for publication November 2, 2015. From the Department of Anesthesiology (M.R.F., K.K., R.R., A.Y., K.L., R.M., G.W.) and Department of Medicine (I.R., M.B.), and Neuroscience Program (M.R.F.), University of Illinois at Chicago, Chicago, Illinois; and Research and Development Service, Jesse Brown Veterans Affairs Medical Center (M.R.F., K.K., R.R., A.Y., K.L., I.R., G.W.), Chicago, Illinois.

Copyright © 2015, the American Society of Anesthesiologists, Inc. Wolters Kluwer Health, Inc. All Rights Reserved. Anesthesiology 2016; 124:428-42

the absence of toxicity, lipid emulsions modulate AMPK in a number of different tissues.¹⁹ Based on this evidence, we hypothesized that bupivacaine-induced cardiac toxicity adversely affects cellular signaling at targets of glucose homeostasis, including Akt and AMPK,⁶ and that recovery with ILE modifies this process.

Materials and Methods

Rats were housed as pairs in the Veterinary Medical Unit at the Jesse Brown Veterans Affairs Medical Center (JBVAMC, Chicago, Illinois). Experiments were conducted under sterile conditions in the Veterinary Medical Unit at the JBVAMC. Protocols were approved by the Institutional Animal Care and Utilization Committee of the JBVAMC (IACUC Protocol No. 12-18).

In Vivo Model

Sprague–Dawley rats ($n = 29$) weighing between 372 and 426 g were induced with isoflurane in a bell jar before we performed a tracheotomy for intubation and maintained them on 1.2 to 1.75% isoflurane for the remainder of the experiment. Animals were instrumented with a carotid catheter to measure blood pressure, bilateral jugular catheters for infusions, and three electrodes to measure electrocardiogram. After a 30-min equilibration period, animals received 10 mg/kg bupivacaine hydrochloride into the left internal jugular over 20 s to produce a transient asystole. A subset of animals also received adjuvant ILE (10 mg/kg, 30% Intralipid®; Baxter Pharmaceuticals, USA). At pre-specified time points (1.5, 5, and 10 min) after injection, animals were sacrificed by rapid cardiac excision. Tissue was immediately frozen in liquid nitrogen. The peritoneum was opened, and the right kidney was removed and frozen in liquid nitrogen as well. Three animals were pretreated 10 min before bupivacaine with 25 µg/kg of IV Wortmannin (Sigma-Aldrich, USA). In addition, a group of animals ($n = 8$) received only 10 ml/kg lipid emulsion (over 1 min, with no bupivacaine) and were sacrificed at 3.5 min after infusion (matched to the 5-min bupivacaine + ILE time point). Tissues were prepared in a similar manner. Physiological data were recorded with LabChart 7.0 (ADInstruments, USA).

Ex Vivo Isolated Hearts

Sprague–Dawley rats ($n = 20$) were anesthetized by intraperitoneal injection of 60 mg/kg sodium pentobarbital (Abbott Laboratories, USA). Animals were heparinized before cardiac excision. Hearts were suspended from a Langendorff apparatus (Radnoti & ADInstruments, USA), cannulated at the aortic root, and perfused by roller pump at a rate of 16 ml/min with Krebs–Henseleit buffer (100 mM NaCl, 4.74 mM KCl, 1.18 mM KH₂PO₄, 1.18 mM MgSO₄, 1.00 mM CaCl₂, 25.00 mM NaHCO₃, 11.50 mM glucose, 4.92 mM pyruvate, and 5.39 mM fumarate), at 37°C and pH 7.40. The buffer was equilibrated with a mixture of

oxygen (95%) and carbon dioxide (5%) by passing through a membrane oxygenator. Pressure was transduced from a latex balloon in the left ventricle and recorded using LabChart 7.0. Drugs were delivered by syringe pump to stop-cocks approximately 2 cm above the aortic valve. Fourteen hearts were randomized to receive nothing ($n = 2$), 500 µM bupivacaine over 30 s ($n = 6$) or 500 µM bupivacaine over 30 s with pretreatment of 50 µM LY294002 (Sigma-Aldrich) over 1 min ($n = 6$). Two minutes after completion of infusion, hearts were flash-frozen to ensure cardiac bupivacaine concentrations were in accordance with previous experiments.²⁰ The remaining six hearts received 20% ILE (10 mg/kg, 20% Intralipid®) over 10 min infused to a 1% final concentration. Samples of left ventricle were harvested immediately before infusion and at 10-min and flash-frozen in liquid nitrogen.

Western Blotting

All procedures were conducted on ice. The apex of heart and apical pole (cortex only) of the left kidney were isolated. Approximately 100 mg of tissue was dissected, washed, and homogenized in 1.5 ml lysis buffer using an Omni Mixer Homogenizer (Omni International, USA). Lysis buffer comprises 18 mM Tris–HCl, 114 mM NaCl, 0.4% sodium deoxycholate, 0.1% sodium dodecyl sulfate, 9 mM sodium pyrophosphate, 0.9 mM sodium fluoride, 9% glycerol, 10% Triton X-100, 10 mM sodium orthovanadate, 1 mM phenylmethanesulfonyl fluoride, and 1 mM dithiothreitol with pH adjusted to 7.4 and supplemented with Roche Complete Mini EDTA-free tablet (Roche Diagnostic Corporation, USA). Samples were spun at 14K rpm for 10 min to remove insoluble tissue and membranes. Total protein concentration was quantified using a Pierce BCA Protein assay (Thermo Scientific, USA) and iMark microabsorbance plate reader (BioRad, USA). Samples were aliquoted into 50 µl portions and refrozen at –80°C. Twenty micrograms of protein were loaded and run on a 4 to 15% mini-PROTEAN® TGX gel (BioRad) and then transferred to nitrocellulose membrane (Thermo Scientific, USA). Membranes were blotted for 30 min with 5% bovine serum albumin Cohn fraction V (Sigma-Aldrich) and washed and incubated with rabbit anti-mouse primary antibodies against pT308-Akt, pS473-Akt, total Akt, pT172 AMPK, pS79 acetyl-CoA carboxylase (ACC), pS21/pS9 glycogen synthase kinase-3α/β, pT421 p70 s6 kinase (p70s6k), pS235 ribosomal protein s6, pS1387 tuberous sclerosis 2 (TSC2), pS612 insulin receptor substrate-1 (IRS1), and total glyceraldehyde-3-phosphate dehydrogenase as loading control (all antibodies from Cell Signaling Technologies, USA). Subsequently, membranes were washed and incubated with goat anti-rabbit IgG linked to horseradish peroxidase-peroxidase (Cell Signaling). Luminescence was induced with Amersham ECL Prime (GE Healthcare Bio-sciences, USA) and exposed under darkroom conditions on care-stream autoradiography film (Sigma-Aldrich). Protein quantification was conducted in ImageJ

(National Institutes of Health, USA). To control for equal loading, samples were quantified and normalized to total glyceraldehyde-3-phosphate dehydrogenase. For AMPK and Akt, phosphoprotein level was subsequently normalized to total protein level. Because time points were early, we did not anticipate major protein synthesis or degradation, and because no changes were observed in total AMPK and Akt, we did not measure (or normalize) total protein levels for other phosphoproteins.

Glycogen Quantification

Glycogen levels were measured with a colorimetric assay (MAK016; Sigma-Aldrich). Left ventricular tissue was isolated, homogenized, and lysed. Lysate was spun and supernatant transferred into tubes for quantification. Glycogen was degraded to glucose with hydrolysis enzyme mix and developed with a colorimetric development enzyme mix. Subsequent coloration coupled to the amount of glycogen in the sample was quantified using an iMark microabsorbance plate reader (BioRad).

Bupivacaine Concentration Fit Curves and Grouping

Fit curves for bupivacaine concentrations in heart and kidney were developed based on data in Fettiplace *et al.*³ In brief, concentration of drug in tissue was plotted against time and fit to a single-phase exponential decay with a y-intercept held at zero. As described in the previous publication, recovery of cardiovascular parameters (carotid flow and blood pressure) is coincident with cardiac bupivacaine concentrations dropping below known inhibitory concentrations for voltage-gated ion channels. In those experiments, carotid flow was depressed when cardiac bupivacaine concentrations were greater than 100 nmol/g but flows recovered less than 100 nmol/g and peaked approximately 50 nmol/g. This provided a grouping mechanic based on a “recovery threshold” that reflects recovery of cardiovascular parameters and myocardial drug concentrations either more than or less than approximately 100 nmol/g. This level is consistent with the half-maximal inhibitory concentration (IC_{50}) of bupivacaine for cardiac sodium channels and cardiac calcium channels. Based on data from previous publications,^{3,21–23} the IC_{50} for sodium and calcium channels translate to tissue concentrations of 87 and 80 μ M, respectively, for both cardiac and kidney tissue. The greater than 100 μ M group includes animals sampled at 1.5 and 5 min and the less than 100 μ M group includes animals at the 10-min time point. Animals receiving ILE in the less than 100 μ M + ILE group were sampled at the 5-min time point. Kidney was used as a control for contractile status. Recovery was ignored, and groups were analyzed based on kidney bupivacaine concentrations greater than 100 μ M.

Statistical Analysis and Power Quantification

Omnibus testing was conducted by two-way ANOVA with matched samples grouped by kinase and time point. *Post hoc*

differences were assessed by Sidak tests to control for multiple comparisons. Groupwise α was set at 0.05. Because data were non-normal with large differences in scale and variance, data were ranked before statistical testing to provide normalization.^{24,25} Physiological and recovery parameters without grouping components were assessed with the double-sided Mann–Whitney U tests. A pilot set of animals in the bupivacaine only group (control, 1, 5, and 10 min), bupivacaine + ILE group (1, 5, and 10 min), and lipid-only group at 5 min were run to make power calculations. For comparisons against baseline, we determined a sample size of eight (four per group) based on a Cohen *d* of 2.8, power = 0.8, and α = 0.05 for bupivacaine comparisons. For the bupivacaine + ILE and ILE alone, we expected a robust effect size but anticipated the need for a larger sample size (10) based on a slightly smaller Cohen *d* (approximately 2.3) due to larger variance of values during recovery. Physiological data and densitometry data are expressed as mean \pm SEM.

Results

Bupivacaine Toxicity Inhibits Akt and Targets Downstream of mTORC1 Signaling in Cardiac Tissue

We used a previously characterized single IV injection model of low-dose bupivacaine toxicity^{3,5,26} to assess kinase phosphorylation and dephosphorylation in cardiac tissue in response to a recoverable dose of bupivacaine. The advantage of this model is that after the rapid onset of asystole, animals recover without further intervention (fig. 1A). The gradual improvement in cardiac output is coincident with cardiac bupivacaine content falling below the IC_{50} for multiple voltage-gated ion channels in the heart (fig. 1B), providing a grouping mechanism based on recovery status and tissue concentration of bupivacaine that reflects the level of channel inhibition (see Materials and Methods: Bupivacaine Concentration Fit Curves and Grouping). Unrecovered (*e.g.*, cardiac bupivacaine greater than 100 μ M) animals from the 1.5- and 5-min time points were anticipated to have cardiac bupivacaine concentrations of 301 ± 23 nmol/g (95% CI) and 152 ± 25 nmol/g (95% CI), respectively. Recovered animals (*e.g.*, cardiac bupivacaine less than 100 μ M) from the 10-min postchallenge time point were expected to have cardiac bupivacaine concentration of 57 ± 21 nmol/g (95% CI). At the 10-min time point when cardiac bupivacaine was less than 100 μ M, rate pressure product (RPP) had improved to $37 \pm 2\%$ of baseline (mean \pm SEM) compared with $15 \pm 6\%$ at the 1.5- and 5-min time points (P = 0.01; fig. 1C).

We examined changes in cellular signaling by Western blotting for phosphoproteins in the insulinergic pathway. We quantified concentrations of Akt phosphorylated at S473 and T308, and the downstream targets glycogen synthase kinase-3 β (GSK-3 β) at S9, p70s6k at T421, ribosomal protein s6 at S235, and feedback phosphorylation of IRS1 at S612 (fig. 1D). Consistent with previous reports,^{7–9} bupivacaine reduced signaling in the Akt pathway with

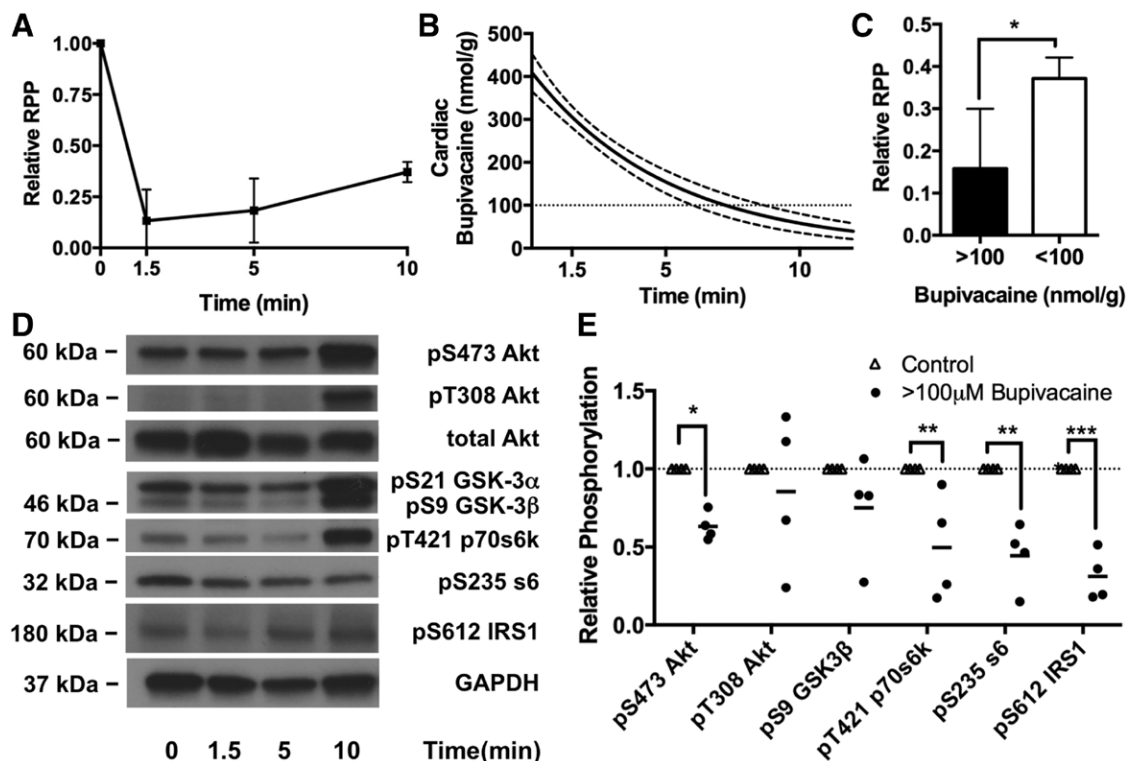


Fig. 1. Cardiac phosphorylation of protein kinase B/Akt and downstream proteins after bupivacaine toxicity. (A) Cardiac output as measured by rate pressure product (RPP = mean arterial pressure \times heart rate) in response to bupivacaine toxicity. (B) Theoretical cardiac bupivacaine (solid line) concentration with 95% CI (dotted lines) based on radiolabel studies (see Materials and Methods: Bupivacaine Concentration Fit Curves and Grouping). (C) Relative RPP difference between groups above ionotropic cation channel (e.g., sodium and calcium) IC_{50} (greater than 100 μ M bupivacaine) and below cation channel IC_{50} (less than 100 μ M bupivacaine), * $P < 0.05$. (D) Western blots of cardiac lysates at different time points during recovery for phosphoproteins in the insulinergic pathway including protein kinase B (Akt) phosphorylated at S473; Akt phosphorylated at T308; total Akt, glycogen synthase kinase-3 α (GSK-3 α) and -3 β (GSK-3 β) phosphorylated at S21 and S9, respectively; p70 s6 kinase (p70s6k) phosphorylated at T421; ribosomal protein s6 (s6) phosphorylated at S235, insulin receptor substrate-1 (IRS1) phosphorylated at S612; and total glyceraldehyde-3-phosphate dehydrogenase (GAPDH) as loading control. (E) Densitometry of cardiac lysates (from "D") comparing control phosphorylation ($n = 4$) to unrecovered animals with greater than 100 μ M of cardiac bupivacaine ($n = 4$); * $P < 0.05$, ** $P < 0.01$, *** $P < 0.001$, Sidak post hoc test.

treatment accounting for 48% of the effect (fig. 1E; two-way matched sample ANOVA interaction $P = 0.0035$, kinase effect $P = 0.0035$, treatment effect $P = 0.0083$, matching $P < 0.0001$). Phosphorylation was decreased on Akt at S473 to $63 \pm 5\%$ (mean \pm SEM, Sidak post-test $P = 0.017$), p70s6k at T421 to $50 \pm 17\%$ ($P = 0.0043$), ribosomal protein s6 at S235 to $44 \pm 11\%$ ($P = 0.0015$), and IRS1 at S612 to $31 \pm 8\%$ ($P = 0.0004$) compared with baseline values. However, targets directly downstream of Pi3k (T308 on Akt and S9 on GSK-3 β) were less consistently affected with reductions on Akt at T308 to $85 \pm 25\%$ of baseline ($P = 0.98$; 95% CI, 0.23 to 1.33) and GSK-3 β at S9 to $75 \pm 17\%$ of baseline ($P = 0.42$; 95% CI, 0.27 to 1.06).

Bupivacaine Toxicity Activates AMPK in Cardiac Tissue

To resolve the discrepancy that targets downstream of the mammalian target of rapamycin complex 1 (mTORC1) including p70s6k and s6 were preferentially affected, we looked to test other signaling targets. Specifically,

5'-adenosine-monophosphate kinase (AMPK) provides a countervailing force at TSC2 that inhibits mTORC1 and downstream targets (fig. 2A) and has been implicated in cellular models of bupivacaine toxicity.^{11,12} We probed for phosphorylation of AMPK at T172 and its downstream targets, ACC at S79, and TSC2 at S1387 (fig. 2B). We again found that treatment accounted for the largest portion of the variation (77%) in groupwise comparison (two-way matched sample ANOVA: interaction $P < 0.0001$, kinase effect $P < 0.0001$, treatment effect $P < 0.0011$, matching $P < 0.0001$). Across all time points, phosphorylation increased to $151 \pm 19\%$ of baseline at T172 on AMPK (Sidak: $P = 0.0001$), $179 \pm 32\%$ of baseline at S79 on ACC ($P = 0.0001$; fig. 2C), and $1,266 \pm 258\%$ of baseline at S1387 on TSC2 ($P = 0.0001$; fig. 2D).

Activation of Insulinergic Signaling during Recovery

We next analyzed the phosphorylation status (of this pathway) during recovery. We found that at the 10-min time

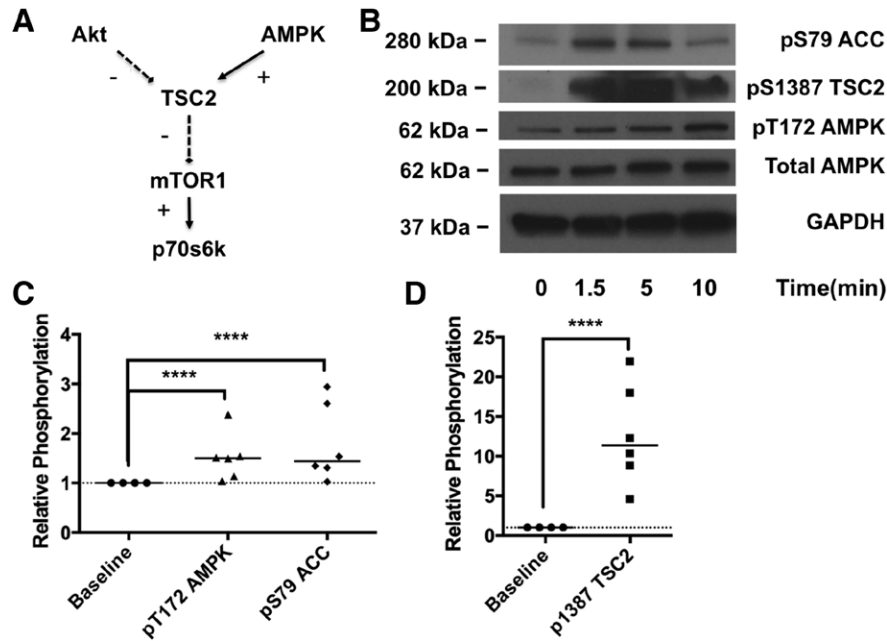


Fig. 2. 5'-Adenosine monophosphate-activated kinase phosphorylation during toxicity. (A) Cellular signaling schematic representation illustrating the convergence of protein kinase B (Akt) and 5'-adenosine monophosphate-activated kinases (AMPK) signaling on the mammalian target of rapamycin complex 1 (mTOR1), which controls downstream targets including p70 s6 kinase (p70s6k). (B) Western blots of cardiac lysates at different time points during recovery for the AMPK pathway including acetyl-CoA carboxylase (ACC) phosphorylated at S79; tuberous sclerosis 2 (TSC2) phosphorylated at S1387; AMPK phosphorylated at T172; and total AMPK and total glyceraldehyde-3-phosphate dehydrogenase (GAPDH) as loading control. (C) Densitometry of phospho-AMPK and phospho-ACC comparing concentrations at baseline ($n = 4$) with concentrations during toxicity ($n = 6$); **** $P < 0.0001$, *post hoc* Sidak test. (D) Densitometry of phospho-TSC2 comparing concentrations at baseline ($n = 4$) with concentrations during toxicity ($n = 6$); * $P < 0.0001$, Sidak *post hoc* test.

point (when cardiac bupivacaine concentrations were less than 100 μM), there was a marked increase in phosphorylation of key signaling proteins above baseline levels (e.g., hyperphosphorylation). This hyperphosphorylation was observed in Akt at S473 to $378 \pm 84\%$ of baseline (Sidak: $P < 0.0001$) and T308 to $390 \pm 64\%$ of baseline ($P < 0.0001$), GSK-3 β at S9 to $293 \pm 50\%$ of baseline ($P = 0.0005$), p70s6k at T421 to $203 \pm 29\%$ of baseline ($P = 0.0002$), and IRS1 at S612 to $186 \pm 37\%$ of baseline ($P < 0.0001$; fig. 3A) in comparison with unrecovered animals (two-way matched subject ANOVA: interaction $P < 0.0001$, kinase effect $P < 0.0001$, recovery effect $P = 0.002$, matching $P < 0.0001$). We further assessed for biochemical changes by examining the cardiac glycogen content in these hearts and found an increase in glycogen from $2.4 \pm 0.17 \mu\text{M/g}$ to $3.4 \pm 0.26 \mu\text{M/g}$ (Mann-Whitney U test, $P = 0.006$; fig. 3B). Both these changes are consistent with a sensitization to canonical insulin signaling caused by the loss of negative feedback to IRS1 (fig. 3C).

Akt Signaling Is Blunted in Kidney

To confirm that the loss of phosphorylation after bupivacaine challenge was not a contractile or flow-dependent phenomenon, we assayed for phosphorylation changes in the kidney, which experiences very high bupivacaine concentrations in this experimental system (fig. 4A) but is not subject to contractile effects. We assessed phosphorylation of Akt at S473

and T308, as well as phosphorylation of the downstream target GSK-3 β at S9 (fig. 4, B and C) at three time points when bupivacaine concentrations were above channel blocking thresholds with an expected concentration of $171 \pm 25 \text{ nmol/g}$ (95% CI). There was a marked treatment-specific effect (two-way ANOVA, treatment $P < 0.0001$, 69% of variation) with no interaction ($P = 0.93$) or kinase ($P = 0.93$) effect. There was a decrease in Akt phosphorylation at S473 to $56 \pm 13\%$ of baseline ($n = 8$, $P = 0.0015$, Sidak post-test), a decrease in Akt phosphorylation at T308 to $62 \pm 11\%$ of baseline ($n = 5$, $P = 0.0012$, Sidak post-test), and a decrease in GSK-3 β phosphorylation at S9 to $42 \pm 18\%$ of baseline ($n = 5$, $P = 0.0041$, Sidak post-test).

Blocking Pi3K Signaling Exacerbates Recovery

We used pharmacological inhibitors to assess whether interfering with this pathway modifies recovery. In the *in vivo* system, we used the irreversible Pi3k inhibitor—Wortmannin (fig. 5A)—to determine whether sensitization to insulin signaling and subsequent activation of Akt is required for recovery. Animals were pretreated with Wortmannin and 10 min later subjected to the standard bupivacaine infusion, sacrificed at 10 min and phosphorylation of targets downstream from Pi3k were assessed (fig. 5B). Treatment with Wortmannin raised blood pressures by approximately 20 mmHg in one animal but did not have any other

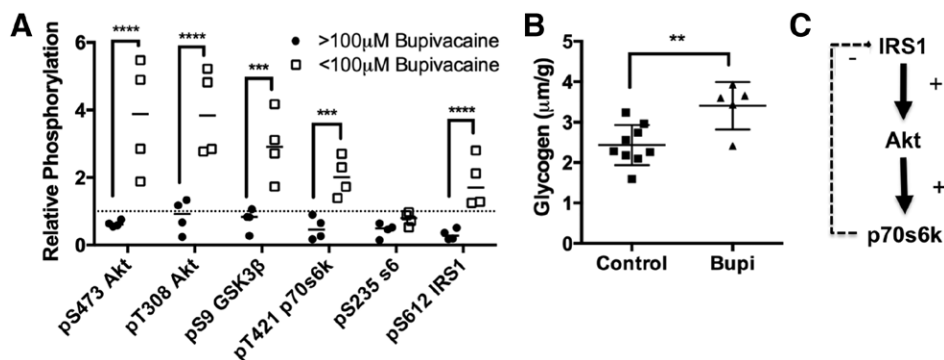


Fig. 3. Recovery-dependent cardiac protein phosphorylation. (A) Densitometry of phosphoproteins in insulinergic pathway in recovered animals with less than 100 μM cardiac bupivacaine ($n = 4$) compared with densitometry during toxicity (greater than 100 μM bupivacaine, $n = 4$); $***P < 0.001$, $****P < 0.0001$, Sidak *post hoc* test. Proteins blotted for include protein kinase B (Akt) phosphorylated at S473; Akt phosphorylated at T308; total Akt, glycogen synthase kinase-3α (GSK-3α) and -3β (GSK-3β) phosphorylated at S21 and S9, respectively; p70 s6 kinase (p70s6k) phosphorylated at T421; ribosomal protein s6 (s6) phosphorylated at S235; insulin receptor substrate-1 (IRS1) phosphorylated at S612; and total glyceraldehyde-3-phosphate dehydrogenase (GAPDH) as loading control. (B) Cardiac glycogen concentration for control hearts ($n = 9$) and bupivacaine-treated hearts in recovery ($n = 5$), $**P = 0.01$ by two-sided *t* test. (C) Schematic representation of feedback pathway underlying sensitization of insulinergic signaling demonstrating how loss of feedback from p70s6k (and other kinases) to IRS1 leads to a sensitization and amplified activation of downstream targets including Akt.

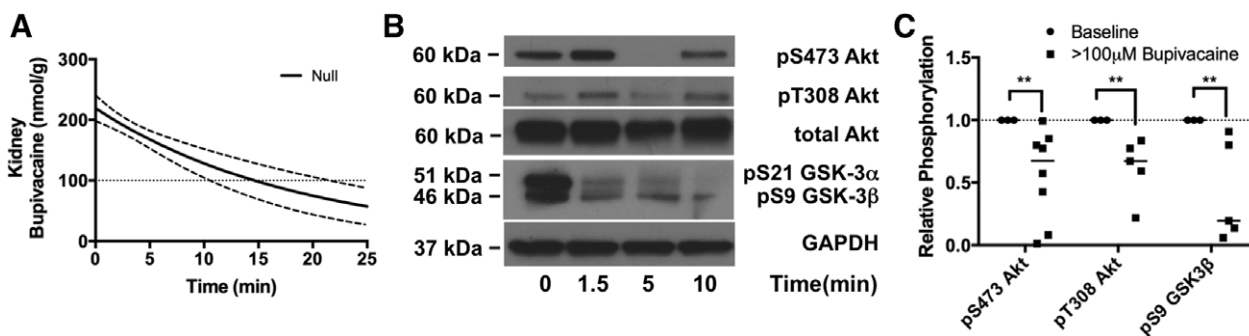


Fig. 4. Protein kinase B/Akt and downstream dephosphorylation is not tissue dependent. (A) Theoretical kidney bupivacaine concentration (solid line) with 95% CI (dotted lines) based on radiolabel studies (see Materials and Methods: Bupivacaine Concentration Fit Curves and Grouping). (B) Western blots of lysates from cortex of kidney at different time points during recovery for protein kinase B (Akt) phosphorylated at S473, Akt phosphorylated at T308, glycogen synthase kinase-3α (GSK-3α) and -3β (GSK-3β) phosphorylated at S21 and S9, respectively, with total glyceraldehyde-3-phosphate dehydrogenase (GAPDH) as loading control. (C) Densitometry of kidney lysate Western blots for Akt at S473 and T308 relative to total Akt and loading control and densitometry of GSK-3β relative to loading control for tissue concentration of bupivacaine greater than sodium channel IC₅₀ (greater than 100 μM bupivacaine) compared with baseline, $**P < 0.01$, Sidak *post hoc* test.

prominent effects. Consistent with the effect of Wortmannin, we found that phosphorylation of proteins was reduced in comparison with the animals that were not treated with Wortmannin (fig. 5C; two-way matched sample ANOVA, treatment effect 74% of variation, $P = 0.0011$, kinase effect $P < 0.0001$, interaction $P = 0.0003$, matching $P < 0.0001$). In addition, Wortmannin blunted recovery from toxicity, reducing cardiac output at 10 min to $12 \pm 8\%$ of baseline in contrast to $37 \pm 2\%$ of baseline in the animals not treated with Wortmannin ($P = 0.03$) (fig. 5D). To ensure that this was a cardiac-specific effect, we tested the effect of the specific PI3K inhibitor LY294002 on bupivacaine toxicity in an isolated heart system with a constant flow state. Animals were acutely treated with LY294002, 1 min before bupivacaine toxicity and then subjected to a bupivacaine challenge.

Time to recovery was not different between groups (fig. 5E), and physiological parameters were not different upon recovery (fig. 5F), but pretreatment with LY294002 significantly delayed the time until the occurrence of asystole, with three animals in the LY group not experiencing asystole until after the bupivacaine infusion was stopped (fig. 5G).

Lipid Emulsion Accelerates Physiological Recovery

Next, we characterized the effect of ILE supplementation on kinase phosphorylation during recovery. Consistent with previous reports,⁵ treatment with ILE accelerated physiological recovery from toxicity (fig. 6A) and within 5 min animals treated with ILE had achieved $98 \pm 7\%$ of baseline RPP compared with untreated animals who were at $18 \pm 9\%$ of baseline (Mann–Whitney U test, $P = 0.002$). Although

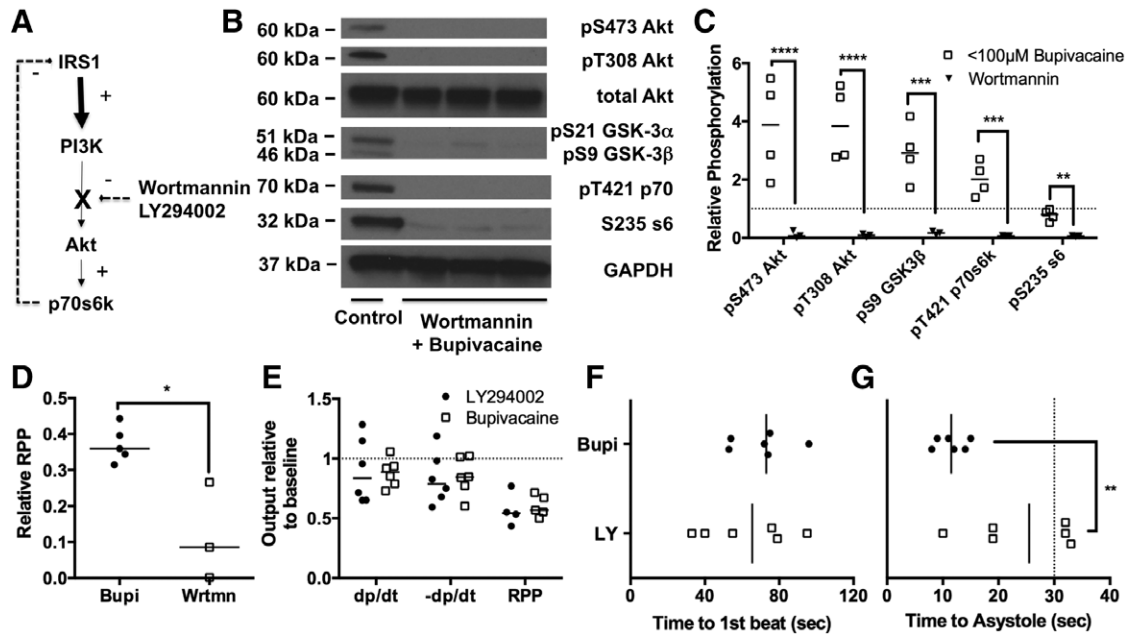


Fig. 5. Blocking signaling exacerbates toxicity. (A) Simplified schematic representation of insulinergic signaling from insulin receptor substrate-1 (IRS1) to phosphoinositol-3-kinase (PI3K) to protein kinase B (Akt) to p70 s6 kinase (p70s6k) with inhibition point by Wortmannin and LY294002 between PI3K and Akt. (B) Western blots of cardiac lysates for 10-min time point for animals pretreated with Wortmannin before bupivacaine infusion. Proteins blotted for include Akt phosphorylated at S473; Akt phosphorylated at T308; total Akt, glycogen synthase kinase-3α (GSK-3α) and -3β (GSK-3β) phosphorylated at S21 and S9, respectively; p70 s6 kinase (p70s6k) phosphorylated at T421; ribosomal protein s6 (s6) phosphorylated at S235; and total glyceraldehyde-3-phosphate dehydrogenase (GAPDH) as loading control. (C) Densitometry of cardiac lysates comparing protein phosphorylation in recovered animals treated with bupivacaine ($n = 4$, less than 100 μM bupivacaine) or bupivacaine and Wortmannin ($n = 3$, Wortmannin); $^{*}P < 0.01$, $^{***}P < 0.001$, $^{****}P < 0.0001$, Sidak *post hoc* test. (D) Relative rate pressure product (RPP = mean arterial pressure \times heart rate) at 10-min for animals recovering from bupivacaine toxicity either pretreated with Wortmannin (Wrtmn) or nothing (Bupi); $^{*}P < 0.05$, Mann-Whitney U test. (E) Physiological parameters including maximal contraction (dp/dt), maximum relaxation (-dp/dt) and RPP from isolated Langendorff hearts at 2-min recovery point after treatment with 500 μM bupivacaine over 30 s. Hearts were either pretreated with 50 μM LY294002 (LY294002) or nothing (bupivacaine). (F) Time to recovery of first beat for hearts from "E" after bupivacaine-induced asystole. (G) Time to asystole for hearts after bupivacaine treatment for hearts in "E."

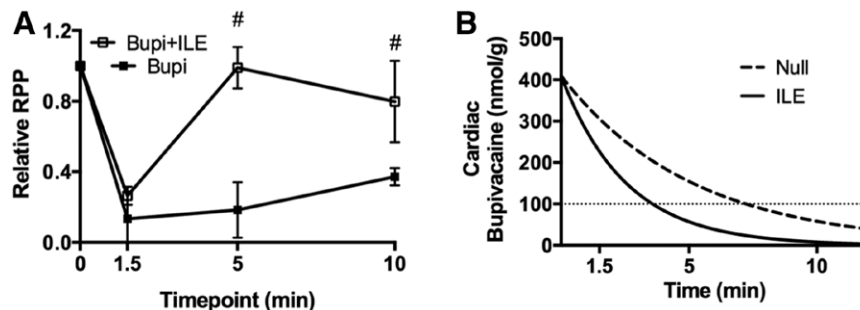


Fig. 6. Cardiac pharmacodynamic and pharmacokinetic effects of lipid emulsion on bupivacaine toxicity. (A) Relative rate pressure product (RPP = mean arterial pressure \times heart rate) in response to bupivacaine toxicity with either nothing (Bupi) or adjuvant 10 ml/kg lipid emulsion (Bupi + ILE), # $P < 0.05$ Mann-Whitney U test. (B) Theoretical cardiac bupivacaine concentration based on previous pharmacokinetic studies for bupivacaine (Null) or bupivacaine and adjuvant IV lipid emulsion (ILE). (See Materials and Methods: Bupivacaine Concentration Fit Curves and Grouping for more details.)

animals in the control group began to recover by 10 min, their cardiac function remained depressed compared with that of the ILE group ($37 \pm 2\%$ vs. $80 \pm 13\%$ compared with baseline RPP for control and ILE, respectively; $P = 0.005$). As with the untreated group, this recovery was coincident

with a time point when cardiac bupivacaine concentrations fell below the IC_{50} for cardiac sodium channels (fig. 6B). For animals receiving ILE in the less than 100 μM + ILE group, the expected cardiac bupivacaine concentration is 59 ± 23 nmol/g (95% CI).

Lipid Emulsion Drives Time-dependent Phosphorylation of Akt during Toxicity but Not Proteins Downstream of mTORC1

Next, we assessed phosphorylation of proteins in the insulin-ergic pathway, including pT308-Akt, pS473-Akt, pS9-GSK-3 β , pT421 p70s6k, pS235 ribosomal protein s6, and pS612 IRS1 at predetermined time points (1.5, 5, and 10 min) during recovery after ILE treatment (fig. 7A). Consistent with observations during spontaneous recovery from bupivacaine toxicity, we observed hyperphosphorylation in the pathway at the 10-min time point for all proteins (not pictured). However, after ILE at the 5-min time point when cardiovascular parameters are recovered and cardiac bupivacaine concentration is below the IC₅₀ for cardiac sodium channels (fig. 6, A and B), we found significant differences from baseline values for phosphorylation of key proteins (fig. 7B, two-way ANOVA, treatment effect $P = 0.004$, kinase effect $P < 0.0001$, interaction $P < 0.0001$). Akt was phosphorylated both at S473 (Sidak: $P = 0.0026$) to $150 \pm 23\%$ of baseline and at T308 ($P = 0.0004$) to $167 \pm 10\%$ of baseline. No change in phosphorylation was seen in S9-GSK-3 β ($98 \pm 14\%$ of baseline). Downstream of mTORC1, we observed dephosphorylation of

p70s6k and s6 and loss of feedback phosphorylation of IRS1: pT421 p70s6k was reduced to $41 \pm 16\%$ ($P = 0.0005$), S235 ribosomal protein s6 reduced to $52 \pm 14\%$ ($P = 0.0002$), and feedback phosphorylation of S612-IRS1 reduced to $45 \pm 12\%$ ($P < 0.0001$) compared with baseline. We confirmed these effects by regressing the data points across time. For the predominant insulin-ergic phosphorylation site on Akt (T308), there was a positive linear regression against time as relative phosphorylation levels of T308 fit to a linear slope ($R = 0.85$) with a non-zero slope of $16 \pm 3\% \text{ min}^{-1}$ ($P < 0.0001$; fig. 7C), and a y-intercept of $100 \pm 2\%$. Downstream of mTORC1, relative phosphorylation levels on threonine 421 of p70s6k also fit to a linear slope ($R = 0.89$) of $28 \pm 6\% \text{ min}^{-1}$ ($P > 0.0001$) but with a y-intercept of $55 \pm 4\%$ that did not include 100% (fig. 7D).

Phosphorylation of TSC2 Downstream of AMPK Remains Consistent through Toxicity Despite Lipid Emulsion Treatment

To assess the source of discordance upstream and downstream of mTORC1, we measured phosphorylation levels of

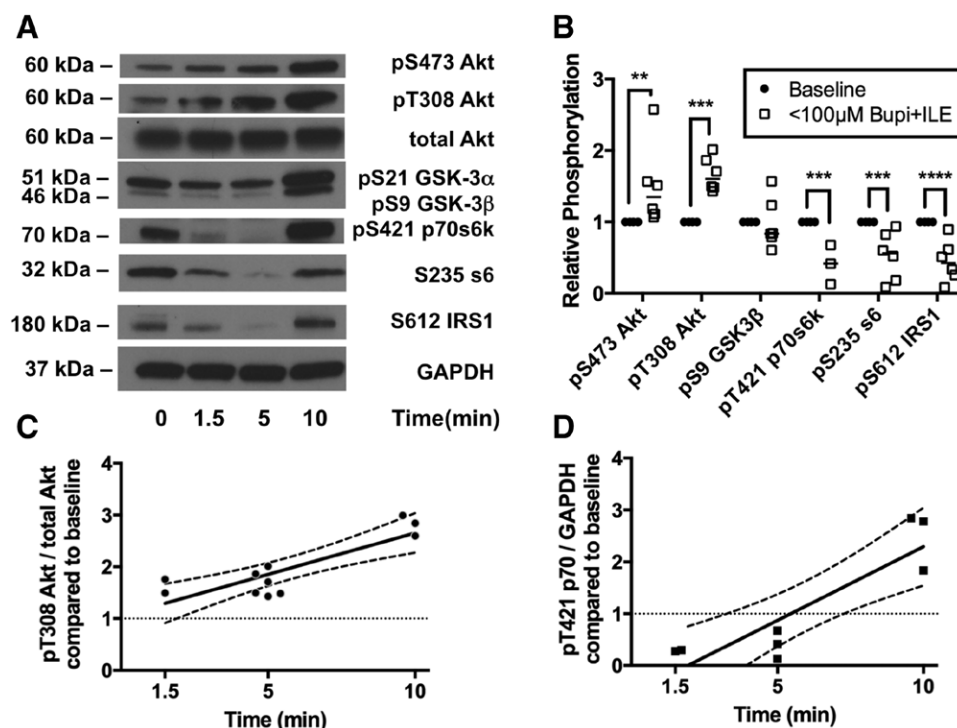


Fig. 7. Activation of protein kinase B/Akt upstream of mammalian target of rapamycin in response to bupivacaine and lipid emulsion. (A) Western blots of cardiac lysates at different time points during recovery from bupivacaine toxicity with adjuvant IV lipid emulsion (ILE) for targets in the insulin-ergic pathway. Proteins blotted for include protein kinase B (Akt) phosphorylated at S473, Akt phosphorylated at T308, total Akt, glycogen synthase kinase-3 α (GSK-3 α) and -3 β (GSK-3 β) phosphorylated at S21 and S9, respectively, p70 s6 kinase (p70s6k) phosphorylated at T421, ribosomal protein s6 (s6) phosphorylated at S235, insulin receptor substrate-1 (IRS1) phosphorylated at S612, and total glyceraldehyde-3-phosphate dehydrogenase (GAPDH) as loading control. (B) Densitometry of cardiac lysates comparing relative phosphorylation level at baseline ($n = 4$) with the relative phosphorylation at the 5-min time point (after both bupivacaine and ILE) when animals are recovered and tissue concentrations are expected to be below sodium channel IC₅₀ (less than 100 μ M Bupi + ILE; $n = 6$; $n = 3$ for p70s6k); ** $P < 0.01$, *** $P < 0.001$, **** $P < 0.0001$, Sidak *post hoc* test. (C) Regression across time of relative phosphorylation level of threonine 308 on Akt. Fit line: pT308-Akt = $0.16 \pm 0.03 \times \text{time} + 1.0 \pm 0.2$ $R = 0.85$. (D) Regression across time of relative phosphorylation level of threonine 421 on p70s6k. Fit line: pS421-p70s6k = $0.28 \pm 0.06 \times \text{time} - 0.55 \pm 0.4$ $R = 0.89$.

AMPK, ACC (fig. 8A), and TSC2 (fig. 8B), in the presence of adjuvant ILE. Consistent with the untreated condition, treatment with the combination of bupivacaine and ILE leads to a robust treatment-specific effect on phosphorylation (two-way ANOVA, $P = 0.0002$) but with no kinase or interaction effects. AMPK was phosphorylated at T172 to $145 \pm 20\%$ of baseline ($P = 0.1125$), and TSC2 was phosphorylated at S1387 to $170 \pm 11\%$ of baseline ($P = 0.0033$); notably, the latter value was similar to that in the context of bupivacaine alone (fig. 8C).

Lipid Emulsion Drives Phosphorylation of Akt in the Absence of Toxicity

Finally, we measured the ability of ILE to change phosphorylation levels of signaling proteins in the absence of toxicity (fig. 9A). For this, we injected animals with ILE (with no accompanying bupivacaine) and sacrificed at a time point matched to the 5-min bupivacaine and ILE time point. At this matched time point, ILE produced a robust treatment effect (two-way ANOVA: $P < 0.0001$) without kinase or interaction effects. We found that ILE rapidly increased phosphorylation of Akt at both T308 (Sidak: $P = 0.0192$) and S473 ($P = 0.0192$; fig. 9B). Furthermore, there was a feedback phosphorylation of IRS1 at S612 ($P = 0.0229$), a phenomenon that is known to contribute to insulin resistance in peripheral skeletal muscle.^{27–29} There were no lipid-induced changes in phosphorylation at downstream targets, including GSK-3 β , p70s6k, or s6. We also found that treatment with ILE alone contributed to glycogen accumulation in the heart (fig. 9C). Next, we checked the effect of ILE on AMPK, ACC, and TSC2 phosphorylation to determine

whether activation of AMPK resulted from ILE or bupivacaine treatment (fig. 9D). Treatment with ILE in the absence of toxicity had no appreciable effects on phosphorylation of AMPK, ACC, or TSC2 (fig. 9E; two-way matched subjects ANOVA, treatment $P = 0.35$, kinase $P = 0.0978$, interaction $P = 0.0978$).

Discussion

We found in a rat model that systemic bupivacaine toxicity is a dynamic insult, whereby fundamentally distinct and separate effects on insulinergic signaling (*i.e.*, Pi3K, Akt, IRS1) and glucose homeostasis (*i.e.*, AMPK, GSK-3 β) occur during induction of toxicity and recovery from it. Our results agree with previous *in vitro* studies, wherein lethal or cytotoxic concentrations of bupivacaine induce dephosphorylation of Akt^{7–9} and phosphorylation of AMPK.^{11,12} Both these kinases integrate signaling at mTORC1 to modulate sensitivity to endogenous insulin³⁰ during recovery from toxicity. As such, we also found that bupivacaine toxicity reduced signaling downstream of Raptor and TSC2 (fig. 10A). The loss of signaling from p70s6k to IRS1 sensitizes insulinergic pathways. Consistent with this, we observed that recovery from bupivacaine-induced cardiac toxicity was associated with hyperactivation of insulinergic targets and an approximately 40% increase in cardiac glycogen stores (fig. 10B), which is associated with better outcomes from cardiac ischemia.³¹ Modulation of glycogen levels by AMPK is asserted to protect against posts ischemic dysfunction.³² The sensitization of signaling serves as a protective mechanism to normalize energy processing in settings where metabolism is impaired. Blocking sensitization with

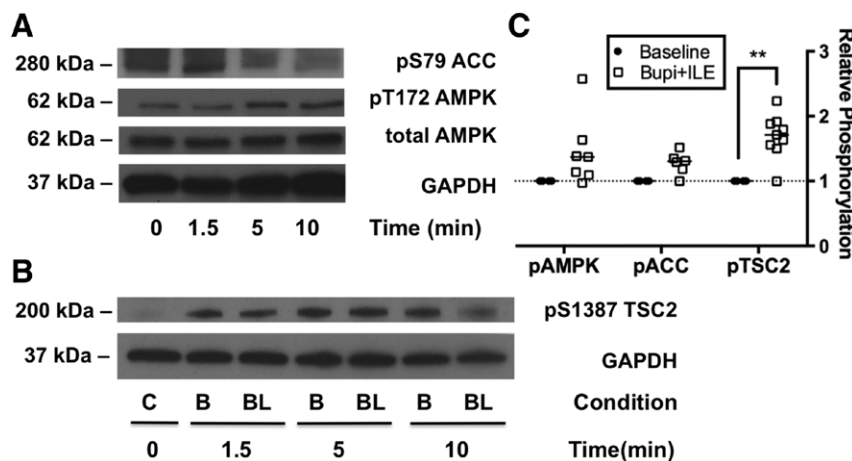


Fig. 8. Persistent activation of 5'-adenosine monophosphate protein-activated kinase signaling, despite the removal of bupivacaine. (A) Western blots of cardiac lysates at different time points during recovery from toxicity with adjuvant IV lipid emulsion (ILE) for acetyl-CoA carboxylase (ACC) phosphorylated at S79, 5'-adenosine monophosphate-activated protein kinase (AMPK) phosphorylated at T172, total AMPK, and total glyceraldehyde-3-phosphate dehydrogenase (GAPDH) as loading control. (B) Western blots of tuberous sclerosis 2 (TSC2) phosphorylated at S1387 and total GAPDH as loading control from cardiac lysates at different time points during recovery from toxicity with bupivacaine (condition = B) and with bupivacaine and adjuvant ILE (condition = BL). (C) Densitometry of phosphoproteins from cardiac lysates comparing relative phosphorylation level of baseline with samples treated with bupivacaine and adjuvant ILE (bupi + ILE; $n = 7$ for pAMPK and pACC, $n = 9$ for pTSC2); ** $P < 0.01$, Sidak *post hoc* test.

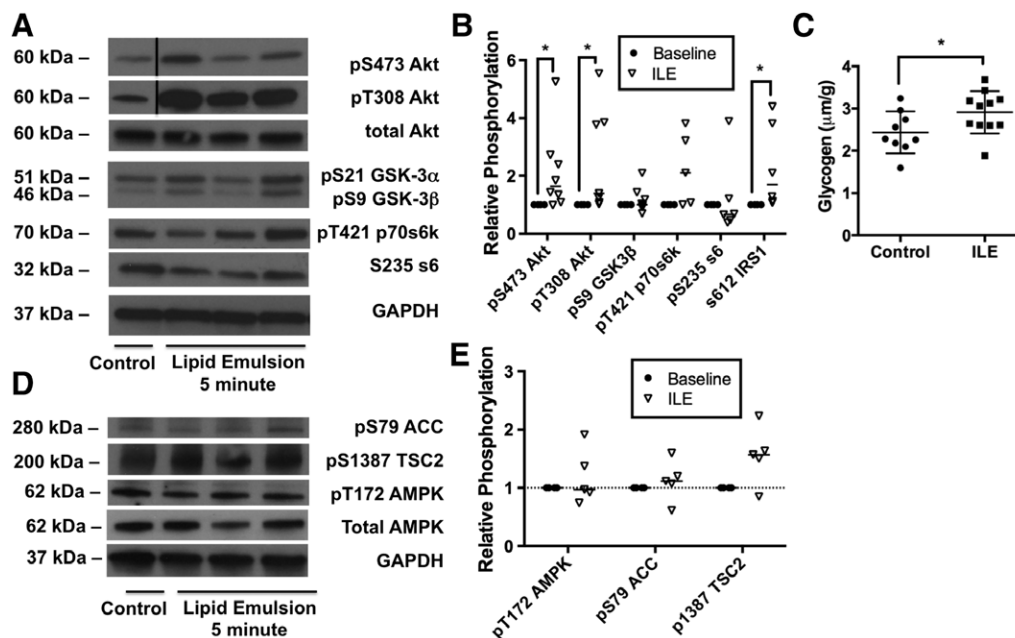


Fig. 9. Rapid activation of insulinergic signaling in response to lipid emulsion in the absence of toxicity. (A) Western blots for targets in the insulinergic pathway from cardiac lysates 3.5 min after 10 ml/kg IV lipid emulsion (ILE, equivalent to 5-min time point in bupivacaine + ILE condition). Proteins blotted for include protein kinase B (Akt) phosphorylated at S473; Akt phosphorylated at T308; total Akt, glycogen synthase kinase-3 α (GSK-3 α) and -3 β (GSK-3 β) phosphorylated at S21 and S9, respectively; p70 s6 kinase (p70s6k) phosphorylated at T421; ribosomal protein s6 (s6) phosphorylated at S235; insulin receptor substrate-1 (IRS1) phosphorylated at S612; and total glyceraldehyde-3-phosphate dehydrogenase (GAPDH) as loading control. (B) Densitometry of cardiac lysates for data in "A" ($n = 5$ to 8); $*P < 0.05$, Sidak *post hoc* test. (C) Cardiac glycogen concentration for control hearts ($n = 9$) and ILE-treated hearts ($n = 11$), $*P = 0.0473$ by two-sided *t* test. (D) Western blots for phosphoproteins in the 5'-adenosine monophosphate-activated protein kinase (AMPK) signaling pathway from cardiac lysates 3.5-min after 10 ml/kg lipid emulsion (no bupivacaine). Proteins blotted for include AMPK phosphorylated at T172, acetyl-CoA carboxylase (ACC) phosphorylated at S79, tuberous sclerosis 2 (TSC2) phosphorylated at S1387, total AMPK, and total GAPDH as loading control. (E) Densitometry of cardiac lysates from "D" comparing relative phosphorylation at baseline ($n = 4$) to levels following ILE ($n = 5$).

Wortmannin, an irreversible inhibitor of Pi3K, interfered with recovery. Transiently blocking Pi3K with the reversible inhibitor—LY20794—provided resistance to toxicity. These findings implicate the importance of this pathway and associated kinases in response to drug toxicity. Wortmannin can also interfere with mTORC1 signaling, so that the importance of the AMPK pathway is reinforced by the findings.

Adjuvant Lipid Emulsion Drives Akt

We found that ILE produced rapid changes to insulinergic signaling at Akt and other targets coincident with recovery from toxicity. Treatment with ILE in the absence of bupivacaine toxicity activated insulin signaling at Akt but had no effect on AMPK (fig. 11A). In combination, bupivacaine and ILE provided concurrent activation of both AMPK and Akt. AMPK blocked mTORC1 and downstream targets (p70, s6, and IRS1), while the addition of ILE induced early rephosphorylation of Akt, upstream of mTORC1 (fig. 11B). One of our more interesting findings was the rapidity with which these systems turned on and off. AMPK, Akt, and downstream targets were significantly altered at our earliest time point (1.5 min) and again by 10 min, when Akt was fully rephosphorylated. Lipid emulsion drives rapid physiological

changes both in the context of toxicity and in its absence that could be mediated by changes in signaling.^{4,33} The involvement of these pathways also points to other treatments for toxicity that could accelerate recovery through modulation of metabolic or signaling pathways.

Local Anesthetics and Insulin Signaling

Local anesthetics are known to modulate energy processing as carnitine deficiency sensitizes animals to bupivacaine toxicity,³⁴ a finding that confirmed the clinical observation that carnitine deficiency predisposes patients to bupivacaine toxicity.^{35,36} Furthermore, local anesthetics inhibit mitochondrial carnitine exchange in experimental models,^{37,38} and supplementation of ATP can overcome bupivacaine toxicity in myocardial cells.³⁹ Beyond energy production, a number of clinical and experimental observations comport with the conclusion that local anesthetics modify insulin signaling. Hypoglycemic or streptozotocin-induced diabetic animals are more sensitive to bupivacaine cardiac toxicity,^{40,41} and insulin provides inotropic support during bupivacaine cardiac toxicity.^{42,43} In nontoxic situations, diabetic rats experience extended block durations independent of neurotoxicity^{44–47} and patients with poorly controlled diabetes experience extended duration of

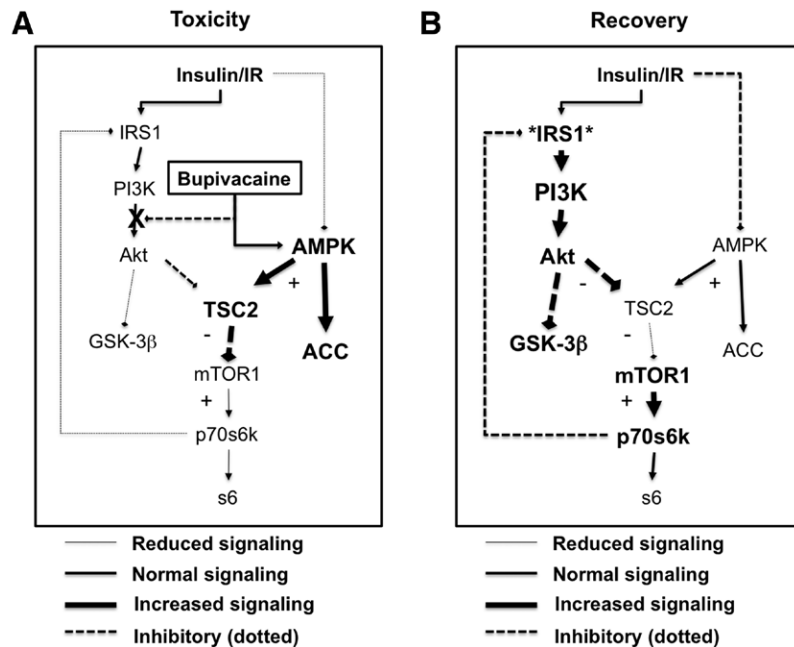


Fig. 10. Schematic representation of induction of and recovery from bupivacaine toxicity. (A) During toxicity, bupivacaine activates 5'-adenosine monophosphate-activated protein kinase (AMPK) with phosphorylation of threonine 172 and blocks protein kinase B (Akt), with the reduction of phosphorylation at serine 473 and some reduced phosphorylation of threonine 308. These two effects converse at tuberous sclerosis 2 (TSC2). AMPK activates TSC2 by phosphorylating it at serine 1387 with a decrease in inhibition of TSC2 by Akt. Kinases downstream of the mammalian target of rapamycin complex 1 (mTOR1) including p70 s6 kinase (p70s6k) and ribosomal protein s6 (s6) will be less activated. Feedback inhibition of insulin receptor substrate-1 (IRS1) by p70s6k is lost leading to sensitization of insulinergic signaling. (B) During recovery, IRS1 is hypersensitized so that at equivalent insulinergic stimulation there will be a hyperactivation of kinases downstream of IRS1 including Akt and glycogen synthase kinase-3 β (GSK-3 β). Both these proteins can control and assist with the recovery of cardiac contractility. AMPK remains phosphorylated and targets downstream of TSC2 and mTOR1 remain unactivated. ACC = acetyl-CoA carboxylase; PI3K = phosphoinositide-3-kinase.

local anesthetic-induced peripheral nerve blocks.^{48–50} Despite the importance of understanding the interaction of local anesthetic effects on diabetic patients,⁵¹ the connection between sensitization to toxicity and glucose handling has previously been incompletely addressed.

Conceivably, improvement in insulin signaling could increase myocardial contractility as both GSK-3 β and Akt interact with contractile proteins downstream.^{52–55} Multiple experimental models have demonstrated that bupivacaine can reduce infarct size in an ischemia–reperfusion model.^{56,57} However, this effect is counterintuitive based on the research demonstrating that bupivacaine and similar amide-linked local anesthetics interfere with antiapoptotic signaling by blocking Akt and downstream targets.^{7–9} A sensitization to insulin signaling during recovery would provide a rational explanation for this effect. As an interesting aside, a clinical trial found that ILE unexpectedly reduced blood glucose levels when used as a treatment for xenobiotic drug overdose.⁵⁸ This finding comports with our observed connections between bupivacaine toxicity, lipid, and insulin signaling.

Exacerbation of Bupivacaine Toxicity

A modification of glucose handling and sensitization of insulinergic signaling provide a new perspective on the

mechanisms underlying physiological recovery from bupivacaine toxicity. Our results demonstrated that Wortmannin exacerbated bupivacaine cardiac toxicity. We know from previous studies that high-dose epinephrine, the classic protein kinase A activator, can also interfere with the recovery from bupivacaine toxicity.⁵⁹ Furthermore, local anesthetic toxicity produces an ischemic-like insult because of mitochondrial uncoupling.^{37,60} It is conceivable that other drugs that exacerbate ischemia–reperfusion injury (opioid receptor antagonists, toll-like receptor 2 antagonists, K_{ATP} channel antagonists, bradykinin antagonists, protein kinase C [PKC] inhibitors, *etc.*) would make bupivacaine toxicity worse. Thus, appropriate controls are needed when studying lipid resuscitation therapy to differentiate worsening of toxicity from inhibition of the beneficial effects of ILE.

Clinical Implications

From a clinical perspective, insulin has been used in the toxicology community for a number of years as a treatment for drug-induced cardiac toxicity. High-dose insulin provides benefit in experimental models of bupivacaine toxicity^{42,43} and is used in emergency rooms for other drug overdoses.⁶¹ In particular, calcium channel blocker (CCB) overdose is associated with a functionally hypoinsulinemic

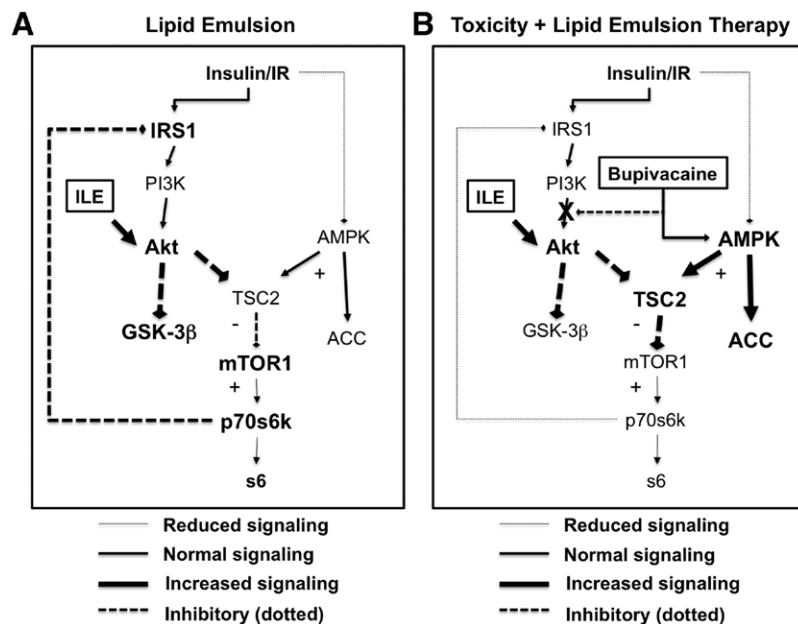


Fig. 11. Schematic representation of contribution of lipid emulsion to the treatment of bupivacaine toxicity. (A) On its own IV lipid emulsion (ILE, 10 ml/kg intralipid) rapidly activates insulinergic signaling in cardiac tissue with the phosphorylation of protein kinase B (Akt) at both threonine 308 and serine 473. This leads to feedback phosphorylation of insulin receptor substrate-1 (IRS1). ILE had no observable effect on 5'-adenosine monophosphate protein-activated kinase (AMPK) or downstream targets including acetyl-CoA carboxylase (ACC) or tuberous sclerosis 2 (TSC2) and did not contribute to inhibition or activation of mammalian target of rapamycin complex 1 (mTOR1), p70 s6 kinase (p70s6k), or ribosomal protein s6 (s6). (B) During toxicity, bupivacaine blocks Akt signaling and activate AMPK signaling with the blockade of downstream proteins including p70s6k and s6 via inhibition of mTOR1 by TSC2. Adjuvant lipid emulsion will cause phosphorylation of Akt at threonine 308 and serine 473. AMPK signaling remains activate due to bupivacaine toxicity with continued loss of signaling downstream mTOR1. With persistent activation, IRS1 does not immediately resensitized. PI3K = phosphoinositide-3-kinase.

state (due to inhibition of insulin secretion) with secondary hyperglycemia. This allows physicians to follow blood glucose as a measure of both the severity of toxicity⁶² and the patient recovery.⁶³ Therefore, clinicians can predict recovery from CCB toxicity by observing dropping blood glucose levels, even before cardiovascular recovery. Experimentally, CCBs cause derangements in Pi3K signaling,^{64,65} a point in common with bupivacaine. Toxicity from tricyclic antidepressants also causes hyperglycemia,⁶⁶ and treatment is associated with increased insulin sensitivity.⁶⁷ Following on this, high-dose insulin therapy is potentially useful for tricyclic toxicity.^{61,68}

Lipid emulsion infusion has complex effects on metabolism, driving insulin resistance *via* diacylglycerol, PKC, and phosphorylation of IRS1.^{27,28} Furthermore, it is known that fatty acids have a rapid uptake phase, which accelerates the cycling of intracellular triacylglycerol stores,⁶⁹ and this driving force is chain length specific and exerts chain length-specific modification on cardiac contractility.⁷⁰ Beyond these basic concepts, the world of lipids in metabolism, signaling, and disease is growing increasingly complex.⁷¹ However, the acute effects of ILE are less well understood. If ILE can effectively modify insulin signaling pathways to counteract detrimental effects of drugs other than local anesthetics, then we may have a better heuristic to decide which drug overdoses

are treatable with ILE. In particular, ILE provides benefit in CCB overdose^{72–74} and tricyclic overdose,^{75,76} but the effect is less clear in β -blocker overdose.⁷⁷ This comports with the aforementioned effects that CCBs and tricyclics have on blood sugar and insulin sensitivity.

Limitations

Our model lacked cardiac compressions, so that rats experienced hypoperfusion and tissue ischemia before hemodynamic recovery. Given that bupivacaine also produces an ischemia-like insult due to mitochondrial uncoupling, our results might reflect changes in Akt and AMPK secondary to ischemia, ATP depletion, and glycolytic switching and not simply bupivacaine toxicity. If this is the case, then results from studies where ILE is used as an adjuvant for I/R injury^{14–17} could be cross-applied to ischemic situations due to local anesthetic toxicity. As noted earlier, this would mean that treatments that adversely impact I/R injury could also worsen recovery from bupivacaine toxicity. In addition, we did not probe all pathways involved in IRS1 sensitization. Both PKC and mitogen-activated protein kinase pathways modulate IRS1 and might do so in the context of bupivacaine toxicity. Furthermore, the inhibitors we used could modify binding of bupivacaine or change entry of drug across the plasma membrane.

Conclusion

Bupivacaine-induced cardiac toxicity activates AMPK and inhibits Akt with integration at TSC2 and loss of feedback from p70s6k to IRS1. This sensitizes cardiac tissue to insulin-ergic signaling during recovery, leading to hyperactivation of both Akt and GSK-3 β and the accumulation of glycogen as cardiac function improves. Preventing hyperactivation with Wortmannin—an irreversible Pi3K inhibitor—exacerbates toxicity and demonstrates the importance of this pathway to recovery. In the absence of toxicity, ILE drives phosphorylation of Akt upstream of mTORC1 but has no effect on the AMPK pathway. During toxicity, ILE also causes an early phosphorylation of Akt without perturbing the activation of AMPK by bupivacaine. As such, AMPK may be the primary actor in regard to toxicity, while Akt may be more involved with recovery. If we use other methods to leverage these protective pathways (*i.e.*, insulinergic sensitization, AMPK activation, and Akt activation), we may be able to optimize treatment for bupivacaine and other drug overdose. Whether similar processes are also operating during other intentional and accidental drug overdose and poisoning merits further research.

Acknowledgments

Dr. Fettiplace was supported by an American Heart Association (Dallas, Texas) predoctoral fellowship 13PRE16810063 and the Department of Anesthesiology at the University of Illinois Hospital and Health Science Center (Chicago, Illinois). Drs. Weinberg and Rubinstein were funded by a U.S. Veterans Administration (Washington, D.C.) Merit Review and a National Institutes of Health CounterACT grant 1U01NS083457-01.

Competing Interests

Dr. Weinberg was awarded a U.S. patent related to lipid resuscitation, is cofounder of ResQ Pharma, Inc. (Chicago, Illinois), with Dr. Rubinstein, and established www.lipidrescue.org, an educational Web site on lipid emulsion as treatment of drug overdose and toxicity. The other authors declare no competing interests.

Correspondence

Address correspondence to Dr. Fettiplace: Department of Anesthesiology (M/C515), University of Illinois Hospital and Health Sciences System, 1740 West Taylor, Chicago, Illinois 60612. mfetti3@uic.edu. Information on purchasing reprints may be found at www.anesthesiology.org or on the mast-head page at the beginning of this issue. ANESTHESIOLOGY's articles are made freely accessible to all readers, for personal use only, 6 months from the cover date of the issue.

References

- Barrington MJ, Kluger R: Ultrasound guidance reduces the risk of local anesthetic systemic toxicity following peripheral nerve blockade. *Reg Anesth Pain Med* 2013; 38:289–97
- Albright GA: Cardiac arrest following regional anesthesia with etidocaine or bupivacaine. *ANESTHESIOLOGY* 1979; 51:285–7
- Fettiplace MR, Lis K, Ripper R, Kowal K, Pichurko A, Vitello D, Rubinstein I, Schwartz D, Akpa BS, Weinberg G: Multimodal contributions to detoxification of acute pharmacotoxicity by a triglyceride micro-emulsion. *J Control Release* 2015; 198:62–70
- Fettiplace MR, Ripper R, Lis K, Lin B, Lang J, Zider B, Wang J, Rubinstein I, Weinberg G: Rapid cardioprotective effects of lipid emulsion infusion*. *Crit Care Med* 2013; 41:e156–62
- Fettiplace MR, Akpa BS, Ripper R, Zider B, Lang J, Rubinstein I, Weinberg G: Resuscitation with lipid emulsion: Dose-dependent recovery from cardiac pharmacotoxicity requires a cardioprotective effect. *ANESTHESIOLOGY* 2014; 120:915–25
- Schultze SM, Hemmings BA, Niessen M, Tschopp O: PI3K/AKT, MAPK and AMPK signalling: Protein kinases in glucose homeostasis. *Expert Rev Mol Med* 2012; 14:e1
- Maurice JM, Gan Y, Ma FX, Chang YC, Hibner M, Huang Y: Bupivacaine causes cytotoxicity in mouse C2C12 myoblast cells: Involvement of ERK and Akt signaling pathways. *Acta Pharmacol Sin* 2010; 31:493–500
- Beigh MA, Showkat M, Bashir B, Bashir A, Hussain Mu, Andrabi KI: Growth inhibition by bupivacaine is associated with inactivation of ribosomal protein S6 kinase 1. *Biomed Res Int* 2014; 2014:831845
- Piegleler T, Votta-Velis EG, Bakhshi FR, Mao M, Carnegie G, Bonini MG, Schwartz DE, Borgeat A, Beck-Schimmer B, Minshall RD: Endothelial barrier protection by local anesthetics: Ropivacaine and lidocaine block tumor necrosis factor- α -induced endothelial cell Src activation. *ANESTHESIOLOGY* 2014; 120:1414–28
- Piegleler T, Votta-Velis EG, Liu G, Place AT, Schwartz DE, Beck-Schimmer B, Minshall RD, Borgeat A: Antimetastatic potential of amide-linked local anesthetics: Inhibition of lung adenocarcinoma cell migration and inflammatory Src signaling independent of sodium channel blockade. *ANESTHESIOLOGY* 2012; 117:548–59
- Lu J, Xu SY, Zhang QG, Lei HY: Bupivacaine induces reactive oxygen species production *via* activation of the AMP-activated protein kinase-dependent pathway. *Pharmacology* 2011; 87:121–9
- Huang L, Kondo F, Goshio M, Feng GG, Harato M, Xia ZY, Ishikawa N, Fujiwara Y, Okada S: Enhanced expression of WD repeat-containing protein 35 *via* CaMKK/AMPK activation in bupivacaine-treated Neuro2a cells. *PLoS One* 2014; 9:e98185
- Lee SJ, Shin TJ, Kang IS, Ha JH, Lee SC, Kim HJ: AMPK attenuates bupivacaine-induced neurotoxicity. *J Dent Res* 2010; 89:797–801
- Rahman S, Li J, Bopassa JC, Umar S, Iorga A, Partownavid P, Eghbali M: Phosphorylation of GSK-3 β mediates intralipid-induced cardioprotection against ischemia/reperfusion injury. *ANESTHESIOLOGY* 2011; 115:242–53
- Li J, Iorga A, Sharma S, Youn JY, Partow-Navid R, Umar S, Cai H, Rahman S, Eghbali M: Intralipid, a clinically safe compound, protects the heart against ischemia-reperfusion injury more efficiently than cyclosporine-A. *ANESTHESIOLOGY* 2012; 117:836–46
- Lou PH, Lucchinetti E, Zhang L, Affolter A, Schaub MC, Gandhi M, Hersberger M, Warren BE, Lemieux H, Sobhi HF, Clanachan AS, Zaugg M: The mechanism of Intralipid®-mediated cardioprotection complex IV inhibition by the active metabolite, palmitoylecarnitine, generates reactive oxygen species and activates reperfusion injury salvage kinases. *PLoS One* 2014; 9:e87205
- Li J, Fettiplace M, Chen SJ, Steinhorn B, Shao Z, Zhu X, Li C, Harty S, Weinberg G, Vanden Hoek TL: Lipid emulsion rapidly restores contractility in stunned mouse cardiomyocytes: A comparison with therapeutic hypothermia. *Crit Care Med* 2014; 42:e734–40
- Zirpoli H, Abdillahi M, Quadri N, Ananthakrishnan R, Wang L, Rosario R, Zhu Z, Deckelbaum RJ, Ramasamy R: Acute

- administration of n-3 rich triglyceride emulsions provides cardioprotection in murine models after ischemia-reperfusion. *PLoS One* 2015; 10:e0116274
19. Anavi S, Ilan E, Tirosh O, Madar Z: Infusion of a lipid emulsion modulates AMPK and related proteins in rat liver, muscle, and adipose tissues. *Obesity (Silver Spring)* 2010; 18:1108–15
 20. Weinberg GL, Ripper R, Murphy P, Edelman LB, Hoffman W, Strichartz G, Feinstein DL: Lipid infusion accelerates removal of bupivacaine and recovery from bupivacaine toxicity in the isolated rat heart. *Reg Anesth Pain Med* 2006; 31:296–303
 21. Coyle DE, Sperelakis N: Bupivacaine and lidocaine blockade of calcium-mediated slow action potentials in guinea pig ventricular muscle. *J Pharmacol Exp Ther* 1987; 242:1001–5
 22. Clarkson CW, Hondeghem LM: Mechanism for bupivacaine depression of cardiac conduction: Fast block of sodium channels during the action potential with slow recovery from block during diastole. *ANESTHESIOLOGY* 1985; 62:396–405
 23. Terasaki T, Pardridge WM, Denson DD: Differential effect of plasma protein binding of bupivacaine on its *in vivo* transfer into the brain and salivary gland of rats. *J Pharmacol Exp Ther* 1986; 239:724–9
 24. Conover WJ, Iman RL: Rank transformation as a bridge between parametric and nonparametric statistics. *Am Stat Assoc* 1981; 35:124–9
 25. Akritas MG: Method in some the rank transform two-factor designs. *Am Stat Assoc* 1990; 85:73–8
 26. Fettiplace MR, Ripper R, Lis K, Feinstein DL, Rubinstein I, Weinberg G: Intraosseous lipid emulsion: An effective alternative to IV delivery in emergency situations. *Crit Care Med* 2014; 42:e157–60
 27. Ravichandran LV, Esposito DL, Chen J, Quon MJ: Protein kinase C-zeta phosphorylates insulin receptor substrate-1 and impairs its ability to activate phosphatidylinositol 3-kinase in response to insulin. *J Biol Chem* 2001; 276:3543–9
 28. Pereira S, Park E, Mori Y, Haber CA, Han P, Uchida T, Stavar L, Oprescu AI, Koulajian K, Ivovic A, Yu Z, Li D, Bowman TA, Dewald J, EL-Benna J, Brindley DN, Gutierrez-Juarez R, Lam TKT, Najjar SM, McKay R a, Bhanot S, Fantus IG, Giacca A: FFA-induced hepatic insulin resistance *in vivo* is mediated by PKC- δ , NADPH oxidase, and oxidative stress. *Am J Physiol Endocrinol Metab* 2014; 307:e34–46
 29. Moschella PC, Rao VU, McDermott PJ, Kuppaswamy D: Regulation of mTOR and S6K1 activation by the nPKC isoforms, PKCepsilon and PKCdelta, in adult cardiac muscle cells. *J Mol Cell Cardiol* 2007; 43:754–66
 30. Witczak CA, Sharoff CG, Goodyear LJ: AMP-activated protein kinase in skeletal muscle: From structure and localization to its role as a master regulator of cellular metabolism. *Cell Mol Life Sci* 2008; 65:3737–55
 31. Scheuer J, Stezoski SW: Protective role of increased myocardial glycogen stores in cardiac anoxia in the rat. *Circ Res* 1970; 27:835–49
 32. Russell RR III, Li J, Coven DL, Pypaert M, Zechner C, Palmeri M, Giordano FJ, Mu J, Birnbaum MJ, Young LH: AMP-activated protein kinase mediates ischemic glucose uptake and prevents postischemic cardiac dysfunction, apoptosis, and injury. *J Clin Invest* 2004; 114:495–503
 33. Fettiplace MR, Weinberg G: The authors reply. *Crit Care Med* 2013; 41:e389–90
 34. Wong GK, Crawford MW: Carnitine deficiency increases susceptibility to bupivacaine-induced cardiotoxicity in rats. *ANESTHESIOLOGY* 2011; 114:1417–24
 35. Weinberg GL, Laurito CE, Geldner P, Pygon BH, Burton BK: Malignant ventricular dysrhythmias in a patient with isovaleric acidemia receiving general and local anesthesia for suction lipectomy. *J Clin Anesth* 1997; 9:668–70
 36. Wong GK, Joo DT, McDonnell C: Lipid resuscitation in a carnitine deficient child following intravascular migration of an epidural catheter. *Anaesthesia* 2010; 65:192–5
 37. Weinberg GL, Palmer JW, VadeBoncouer TR, Zuechner MB, Edelman G, Hoppel CL: Bupivacaine inhibits acylcarnitine exchange in cardiac mitochondria. *ANESTHESIOLOGY* 2000; 92:523–8
 38. Fettiplace MR, Pichurko A, Ripper R, Lin B, Kowal K, Lis K, Schwartz D, Feinstein DL, Rubinstein I, Weinberg G: Cardiac depression induced by cocaine or cocaethylene is alleviated by lipid emulsion more effectively than by sulfobutylether- β -cyclodextrin. *Acad Emerg Med* 2015; 22:508–17
 39. Eledjam JJ, de La Coussaye JE, Brugada J, Bassoul B, Gagnol JP, Fabregat JR, Massé C, Sassine A: *In vitro* study on mechanisms of bupivacaine-induced depression of myocardial contractility. *Anesth Analg* 1989; 69:732–5
 40. Imai M, Chang KS, Tanz RD, Stevens WC, Kemmotsu O: [Enhanced myocardial depression from bupivacaine in diabetic rats]. *Masui* 1991; 40:868–72
 41. Lu GP, Schwalbe SS, Marx GF, Batiller G, Limjoco R: Hypoglycemia enhances bupivacaine-induced cardiotoxicity in the rat. *J Anesth* 1992; 6:255–61
 42. Stehr SN, Pexa A, Hannack S, Heintz A, Heller AR, Deussen A, Koch T, Hübner M: Insulin effects on myocardial function and bioenergetics in L-bupivacaine toxicity in the isolated rat heart. *Eur J Anaesthesiol* 2007; 24:340–6
 43. Kim JT, Jung CW, Lee KH: The effect of insulin on the resuscitation of bupivacaine-induced severe cardiovascular toxicity in dogs. *Anesth Analg* 2004; 99:728–33
 44. Lirk P, Flatz M, Haller I, Hausott B, Blumenthal S, Stevens MF, Suzuki S, Klimaschewski L, Gerner P: In Zucker diabetic fatty rats, subclinical diabetic neuropathy increases *in vivo* lidocaine block duration but not *in vitro* neurotoxicity. *Reg Anesth Pain Med* 2012; 37:601–6
 45. Lirk P, Verhamme C, Boeckh R, Stevens MF, Ten Hoope W, Gerner P, Blumenthal S, de Girolami U, van Schaik IN, Hollmann MW, Picardi S: Effects of early and late diabetic neuropathy on sciatic nerve block duration and neurotoxicity in Zucker diabetic fatty rats. *Br J Anaesth* 2015; 114:319–26
 46. Kroin JS, Buvanendran A, Tuman KJ, Kerns JM: Effect of acute *versus* continuous glycemic control on duration of local anesthetic sciatic nerve block in diabetic rats. *Reg Anesth Pain Med* 2012; 37:595–600
 47. Kalichman MW, Calcutt NA: Local anesthetic-induced conduction block and nerve fiber injury in streptozotocin-diabetic rats. *ANESTHESIOLOGY* 1992; 77:941–7
 48. Cuvillon P, Reubrecht V, Zoric L, Lemoine L, Belin M, Ducombs O, Birenbaum A, Riou B, Langeron O: Comparison of subgluteal sciatic nerve block duration in type 2 diabetic and non-diabetic patients. *Br J Anaesth* 2013; 110:823–30
 49. Sertoz N, Deniz MN, Ayanoglu HO: Relationship between glycosylated hemoglobin level and sciatic nerve block performance in diabetic patients. *Foot Ankle Int* 2013; 34:85–90
 50. Gebhard RE, Nielsen KC, Pietrobon R, Missair A, Williams BA: Diabetes mellitus, independent of body mass index, is associated with a “higher success” rate for supraclavicular brachial plexus blocks. *Reg Anesth Pain Med* 2009; 34:404–7
 51. Williams BA, Murinson BB, Grable BR, Orebaugh SL: Future considerations for pharmacologic adjuvants in single-injection peripheral nerve blocks for patients with diabetes mellitus. *Reg Anesth Pain Med* 2009; 34:445–57
 52. Sugden PH, Fuller SJ, Weiss SC, Clerk A: Glycogen synthase kinase 3 (GSK3) in the heart: A point of integration in hypertrophic signalling and a therapeutic target? A critical analysis. *Br J Pharmacol* 2008; 153(suppl 1):S137–53
 53. Kirk JA, Holewinski RJ, Kooij V, Agnetti G, Tunin RS, Witayavanitkul N, de Tombe PP, Gao WD, Van Eyk J, Kass DA: Cardiac resynchronization sensitizes the sarcomere to calcium by reactivating GSK-3 β . *J Clin Invest* 2014; 124:129–38

54. Gao MH, Tang T, Guo T, Miyanochara A, Yajima T, Pestonjamas K, Feramisco JR, Hammond HK: Adenylyl cyclase type VI increases Akt activity and phospholamban phosphorylation in cardiac myocytes. *J Biol Chem* 2008; 283:33527–35
55. Cittadini A, Monti MG, Iaccarino G, Di Rella F, Tschlis PN, Di Gianni A, Strömer H, Sorriento D, Peschle C, Trimarco B, Saccà L, Condorelli G: Adenoviral gene transfer of Akt enhances myocardial contractility and intracellular calcium handling. *Gene Ther* 2006; 13:8–19
56. Ross JD, Ripper R, Law WR, Massad M, Murphy P, Edelman L, Conlon B, Feinstein DL, Palmer JW, DiGregorio G, Weinberg GL: Adding bupivacaine to high-potassium cardioplegia improves function and reduces cellular damage of rat isolated hearts after prolonged, cold storage. *ANESTHESIOLOGY* 2006; 105:746–52
57. Bouwman RA, Vreden MJ, Hamdani N, Wassenaar LE, Smeding L, Loer SA, Stienen GJ, Lamberts RR: Effect of bupivacaine on sevoflurane-induced preconditioning in isolated rat hearts. *Eur J Pharmacol* 2010; 647:132–8
58. Taftachi F, Sanaei-Zadeh H, Sepehrian B, Zamani N: Lipid emulsion improves Glasgow coma scale and decreases blood glucose level in the setting of acute non-local anesthetic drug poisoning—A randomized controlled trial. *Eur Rev Med Pharmacol Sci* 2012; 16(suppl 1):38–42
59. Hiller DB, Gregorio GD, Ripper R, Kelly K, Massad M, Edelman L, Edelman G, Feinstein DL, Weinberg GL: Epinephrine impairs lipid resuscitation from bupivacaine overdose: A threshold effect. *ANESTHESIOLOGY* 2009; 111:498–505
60. Hiller N, Mirtschink P, Merkel C, Knels L, Oertel R, Christ T, Deussen A, Koch T, Stehr SN: Myocardial accumulation of bupivacaine and ropivacaine is associated with reversible effects on mitochondria and reduced myocardial function. *Anesth Analg* 2013; 116:83–92
61. Holger JS, Engebretsen KM, Marini JJ: High dose insulin in toxic cardiogenic shock. *Clin Toxicol (Phila)* 2009; 47:303–7
62. Levine M, Boyer EW, Pozner CN, Geib AJ, Thomsen T, Mick N, Thomas SH: Assessment of hyperglycemia after calcium channel blocker overdoses involving diltiazem or verapamil. *Crit Care Med* 2007; 35:2071–5
63. Boyer EW, Duic PA, Evans A: Hyperinsulinemia/euglycemia therapy for calcium channel blocker poisoning. *Pediatr Emerg Care* 2002; 18:36–7
64. Bechtel LK, Haverstick DM, Holstege CP: Verapamil toxicity dysregulates the phosphatidylinositol 3-kinase pathway. *Acad Emerg Med* 2008; 15:368–74
65. Benzeroual K, Pandey SK, Srivastava AK, van de Werve G, Haddad PS: Insulin-induced Ca^{2+} entry in hepatocytes is important for PI 3-kinase activation, but not for insulin receptor and IRS-1 tyrosine phosphorylation. *Biochim Biophys Acta* 2000; 1495:14–23
66. Khoza S, Barner JC: Glucose dysregulation associated with antidepressant agents: An analysis of 17 published case reports. *Int J Clin Pharm* 2011; 33:484–92
67. Weber-Hamann B, Gilles M, Lederbogen F, Heuser I, Deuschle M: Improved insulin sensitivity in 80 nondiabetic patients with MDD after clinical remission in a double-blind, randomized trial of amitriptyline and paroxetine. *J Clin Psychiatry* 2006; 67:1856–61
68. Kerns W II: Management of beta-adrenergic blocker and calcium channel antagonist toxicity. *Emerg Med Clin North Am* 2007; 25:309–31; abstract viii
69. Carley AN, Bi J, Wang X, Banke NH, Dyck JR, O'Donnell JM, Lewandowski ED: Multiphasic triacylglycerol dynamics in the intact heart during acute *in vivo* overexpression of CD36. *J Lipid Res* 2013; 54:97–106
70. Lahey R, Wang X, Carley AN, Lewandowski ED: Dietary fat supply to failing hearts determines dynamic lipid signaling for nuclear receptor activation and oxidation of stored triglyceride. *Circulation* 2014; 130:1790–9
71. Carley AN, Taegtmeier H, Lewandowski ED: Matrix revisited: Mechanisms linking energy substrate metabolism to the function of the heart. *Circ Res* 2014; 114:717–29
72. Liang CW, Diamond SJ, Hagg DS: Lipid rescue of massive verapamil overdose: A case report. *J Med Case Rep* 2011; 5:399
73. Tebbutt S, Harvey M, Nicholson T, Cave G: Intralipid prolongs survival in a rat model of verapamil toxicity. *Acad Emerg Med* 2006; 13:134–9
74. Bania TC, Chu J, Perez E, Su M, Hahn IH: Hemodynamic effects of intravenous fat emulsion in an animal model of severe verapamil toxicity resuscitated with atropine, calcium, and saline. *Acad Emerg Med* 2007; 14:105–11
75. Harvey M, Cave G: Intralipid outperforms sodium bicarbonate in a rabbit model of clomipramine toxicity. *Ann Emerg Med* 2007; 49:178–85, 185.e1–4
76. Engels PT, Davidow JS: Intravenous fat emulsion to reverse haemodynamic instability from intentional amitriptyline overdose. *Resuscitation* 2010; 81:1037–9
77. Harvey M, Cave G, Lahner D, Desmet J, Prince G, Hopgood G: Insulin *versus* lipid emulsion in a rabbit model of severe propranolol toxicity: A pilot study. *Crit Care Res Pract* 2011; 2011:361737